International Journal of Engineering and Geosciences
https://dergipark.org.tr/en/pub/ijeg
e-ISSN 2548-0960

Assessment of latest global gravity field models by GNSS/Levelling Geoid

Nazan Yılmaz *1

1Karadeniz Technical University, Department of Geomatics Engineering, Türkiye

Keywords
GGMs
GNSS/Levelling
Geoid
Statistical values

Research Article
DOI: 10.26833/ijeg.1070042

Received: 08.02.2022
Accepted: 24.06.2022
Published: 19.10.2022

Abstract

This paper focuses on making a comparing of GNSS/Levelling data and data obtained from global geopotential models. For comparison, geoid undulations obtained by GNSS/Levelling method and geoid undulations obtained from global geopotential models have been used. As global geopotential models, SGG-UGM-2, XGM2019e_2159, GO_CONS_GCF_2_TIM_R6e, ITSG-Grace2018s, EIGEN-GRGS.RL04.MEAN-FIELD, GOCO06s, GO_CONS_GCF_2_TIM_R6, GO_CONS_GCF_2_DIR_R6 GGMs are used. The data sets used in the improvements of the models are altimetry, satellite, location data and topography. The disparities between the geoid undulations obtained from the GNSS/Levelling method and geoid undulations obtained from global geoid models have been taken. Some statistical criteria for these differences have been calculated. These criteria, such as smallest, biggest, average, standard deviation, Root Mean Square RMS statistical values of deviations between GNSS/Levelling geoid and global geopotential models, are taken into consideration when comparing the models. According to the comparison, the global gravity field model that best fits the GNSS/Levelling is selected.

1. Introduction

Spheric harmonic expansion is a widely performed presentment the earth gravity field. This presentment is meaned by potential coefficients in the spheric harmonic expansion of the field determined using the elements/parameters of the field measured at the earth's surface and/or in extraterrestrial space. The International Center for Earth Models of Gravity (ICGEM) publishes developed Global Gravity Field Models (GGMs) in time [1].

Because of the technological advances in working the earth's gravity field, latest GGMs's precision studies for diverse regions are of trend attention. Satellite gravimetric tasks bottomed on satellite-to-satellite observing and gradiometry make it potential to get big scale properties of the Earth's gravity field, defined with spheric harmonics [2].

Global geopotential models of spherical harmonic coefficients are used to determine the external gravitational field of the Earth. These coefficients are derived from satellite orbit perturbations, terrestrial gravity anomalies and altimeter data. Hundreds of thousands of coefficients and standard deviation values for these coefficients are estimated from millions of observations [3].

GGMs have been developed primarily as satellite-only models containing data from LAGEOS, CHAMP, GRACE, and GOCE, or qua composite models that combine satellite observations with terrestrial, aerial, ship-sourced gravity data, altitude data, and satellite altimetry measurements a comprehensive gravitational field by clarified spatial resolution [4].

Earth's gravity potential on a universal measure and in too great solution is an essential precondition for a variety of geodetic, geophysical and oceanographic research as well practices. Over the last 50 years, there have been developments and corrections in primary gravity modeling hypothesis as parallel the attendance of more precise and full data and developments in the computational facilities existing for digital modeling works [5].

ICGEM website (http://icgem.gfz-potsdam.de/tom_longtime) is published resolutions of gravity field models containing gravity information from special satellites [6].

Special gravity missions have reformed information of the Earth gravity field. CHAMP satellite was started on

* **Corresponding Author**

*(n_berber@ktu.edu.tr) ORCID ID 0000-0002-0615-8218

Cite this article

Yılmaz, N. (2023). Assessment of latest global gravity field models by GNSS/Levelling Geoid. International Journal of Engineering and Geosciences, 8(2), 111-118

July 15, 2000. It is composed the primary gravity field mission to carry a GPS receiver by permanent 3D following capacity as well a sensitive accelerometer to measure non-gravity beeves. The GOCE satellite was perfectly started on March 17, 2009 and began its operating stage in September 2009. The mission target, stated qua cumulative geoid precision, is a mistake of 1-2 cm at 200 harmonic degrees, corresponding to a half wavelength of about 100 [7].

GRACE satellite was started in March 2002 beneath the NASA Earth System Science Pathfinder Program. GRACE is jointly implemented by the NASA and German Aerospace Center. The primary instrument on the twin GRACE satellites is the K-Band Ranging system (KBR) that observes the intersatellite range to a precision of a few microns. This is the fundamental measurement for the GRACE gravity recovery [8].

GRACE has ensured advanced measurements of worldwide massif flow that have conduced major to mentality of big-scale varies in polar ice, groundwater preservation and ocean massif dispersion. Most of these results are obtained from the analysis of spheric gravity fields solved in terms of spheric harmonic fundamental functions. Nevertheless, free harmonic solutions from GRACE normally suffer from bad traceable gradients, outcoming from "stripes" which are traditionally extracted through experimental smoothing and/or "banding" algorithms [9].

GOCE, GRACE and GRACEFO satellites have been obtained wide developments in the grade of GGMs by solving satellite following, accelerometry, and gradiometry. Gravity field's particulars can be withdrawed handling a composition of satellite reproduced measurements and terrestrial gravity measurements with the inclusion of those measured on flitting platforms [10].

Global Navigation Satellite System (GNSS) has been commonly used in several scientific and engineering applications including positioning, navigation, and time transfer for several decades [11]. There are mainly two different orbital information, namely broadcast ephemerides and IGS final ephemerides used in the GPS positioning. The broadcast ephemerides used in practice and real time are obtained through assessments derived from the observations from the USA GPS reference stations. Broadcast ephemerides are formed (depending on GPS week) from satellite information and the accuracies they provide are adequate in many GPS applications [12].

Global positioning systems can be described as revolution today. These systems can be used in determining the approximate location of any object, navigating the means of transportation, in many measuring processes and in many areas that will make life easier [13]. When determining point positions with GNSS, it should be paid attention to both GNSS measurement errors and noise affecting GNSS frequencies. While GNSS measurement errors can be reduced with an appropriate measurement method, the noise affecting GNSS signals are resolved as a result of analyzes [14].

Global Navigation Satellite Systems (GNSS), scientific research, as well as commercial and non-commercial applications has gained great importance. GPS from America, GLONASS from Russia, BEIDOU from China and GALILEO from Europe provided convenience to the user on a global scale in the location determination issues thanks to Satellite systems's (GNSS) modernization and rapid development [15].

2. Global geopotential models

In this paper, SGG-UGM-2, XGM2019e_2159, GO_CONS_GCF_2_TIM_R6e, ITSG-Grace2018s, EIGEN-GRGS.RL04.MEAN-FIELD, GOCO06s, GO_CONS_GCF_2_TIM_R6, GO_CONS_GCF_2_DIR_R6 models have been used.

SGG-UGM-2 has 5′ × 5′ spatial resolution. It is up to degree 2190 and order 2159. It combines the GOCE SGG and SST-hl measurements, ITSG-Grace2018 NEQ system, satellite marine gravity anomalies as well continental gravity information reproduced from EGM2008 [5].

XGM2019e is a unified GGM symbolized by spheroidal harmonics up to 5399 degrees and orders suitable for 2′ (~4 km) spatial resolution. Combination of satellite data with gravity measurements is made usage complete normal equations up to 719 degrees and orders (15') [16].

GO_CONS_GCF_2_TIM_R6e is an expanded type of the satellite only GGM TIM_R6. TIM_R6 contains extra-terrestrial gravity field measurements over polar gap fields of the GOCE [17].

ITSG-Grace2018 is a GRACE's latest sets of gravity field resolutions. It is based on reprocessed GRACE measurement information (L1B RL03) and the recent atmosphere and ocean softening product (AOD1BRL06) [18].

EIGEN-GRGS.RL04.MEAN-FIELD which is based on CNES/GRGS RL04 is existing for the GRACE 2002 and 2016 time period. Extrapolated terms before August 2002 and after May 2016 are based on global fits of monthly coefficients of GRACE information [19].

GOCO06s is the last satellite specific GGM calculated by GOCO. Various observation methods is key in supplying nonstop high precision and the top probable spatial resolution of the Earth's gravity field. The full published dataset of GOCO06s occurs of a static gravity field solution of up to 300 degrees and orders [20].

GO_CONS_EGM_TIM_RL06 has reckoned qua a successor of the RL05 model issued in 2014. It tracks the philosophy of the former GOCE time models with the fundamental opinion that it is based on GOCE measurements only. It is ensured qua a spherical harmonic expansion, cutted at degree 300.

GO_CONS_EGM_TIM_RL06 was calculated qua the heir to the RL05 model issued in 2014. It is based on the reworked gravity gradients of the GOCE satellite and handling improved working touch. It is cutted at 300 degrees as a spheric harmonic expansion [21].

GO_CONS_GCF_2_DIR_R6 is the European Space Agency's Version 6 GOCE gravity field model. It is completed integration of GOCE-Satellite Gravity Gradiometry, GRACE and Satellite Laser Distance following information, ensuring both perfect orbits are compatible and Global Positioning System outcomes. It is a fixed universal only satellite GGM with d/o of 300 [22].

Table 1 shows global gravity models and their data, resolution and year. In this table, A represents altimetry, S represents satellite, G is for location data and T represents topography.

N is geoid height and it can be represented by spheric harmonic parameters using Eq. 1:

where (θ, λ) co-latitude and longitude of the calculation dot and R is the Earth's mean radius, $\bar{P}_{lm}$ is the associated Legendre polynomials, $\bar{C}_{lm}$ and $\bar{S}_{lm}$ are the spheric harmonic coefficients as l degree and m order.

$$N(\theta,\lambda) \approx R \sum_{l=2}^{i_{max}} \sum_{m=0}^{l} \bar{P}_{lm}(sin\theta)[\bar{C}_{lm}cosm\lambda + \bar{S}_{lm}sinm\lambda) \quad (1)$$

Table 1. Recent Global Geopotential Models

Model	Data	Max. Resolution (Degree)	Year
SGG-UGM-2	A, EGM2008, Grace), S(Goce)	2190	2020
XGM2019e_2159	A, G, S(GOCO06s), T	2190	2019
GO_CONS_GCF_2_TIM_R6e	G (Polar), S(Goce)	300	2019
ITSG-Grace2018s	S(Grace)	200	2019
EIGEN-GRGS.RL04.MEAN-FIELD	S	300	2019
GOCO06s	S	300	2019
GO_CONS_GCF_2_TIM_R6	S(Goce)	300	2019
GO_CONS_GCF_2_DIR_R6	S	300	2019

3. Study area and application

In the study, 30 points belonging to Turkey National Basic GNSS Network (TUTGA-99A) were used. The ellipsoidal heights of these points in the TUTGA-99 coordinate system are directly determined by GNSS measurements, and the orthometric heights are the points determined directly or indirectly in the Turkish National Vertical Control Network-1999 datum. You can see these points' distribution in Figure 1. In this paper, these points are named as test points.

Figure 1. Locations of test points

3.1. Application

The geoid undulations according to global geopotential models were interpolated by using user-defined points in ICGEM web page. The Kriging interpolation method as interpolation technique and WGS84 as reference system was used in these calculations.

Differences of geoid undulations obtained from global geopotential models and GNSS/Levelling have been shown in Table 2.

Differences of geoid height values and geoid undulations obtained from global geopotential models and GNSS/Levelling have been shown in Figure 2,3,4,5,6,7,8 and 9.

The differences between the Global Geopotential Models and GNSS/Levelling were calculated using Eq. 2.

$$\Delta N = N_{GNSS/Lev} - N_{GGM} \quad (2)$$

In this equation, ΔN is the geoid height differences, $N_{GNSS/Lev}$ is the geoid height calculated from GNSS/levelling and N_{GGM} is the geoid height calculated from GGMs. For the statistical examination of geoid height differences, minimum, maximum, mean and standard deviation values of ΔN are defined. In addition, the root mean square (RMS) values were calculated using Eq. 3.

$$RMS = \pm\left[(\sum_{i=1}^{k} \Delta N^2_{GPS/Niv-GM})/k \right]^{1/2} \quad (3)$$

Where k is the number of the test points as 30.

The statistical information on the difference between geoid undulations obtained from GGMs and geoid undulations obtained from GNSS/levelling has been shown in Table 3.

Table 2. Differences of geoid undulations

N. N.	GNSS/Lev.-EIGEN-GRGS.RL04	GNSS/ Lev.-GO_CONS_GCF_2_DIR_R6	GNSS/ Lev.-GO_CONS_GCF_2_TIM_R6	GNSS/ Lev.-GO_CONS_GCF_2_TIM_R6e	GNSS/ Lev. -GOCO06s	GNSS/ Lev. -ITSG-Grace2018s	GNSS/ Lev. -SSG-UGM-2	GNSS/ Lev. -XGM2019e_2159
1	-0.173	-0.099	-0.090	-0.100	-0.088	-0.348	0.022	0.083
2	0.572	0.484	0.547	0.554	0.559	0.498	0.648	0.562
3	0.043	-0.057	-0.070	-0.071	-0.066	0.329	0.035	0.041
4	0.017	0.190	0.196	0.187	0.197	0.216	0.046	0.015
5	-0.460	-0.533	-0.544	-0.540	-0.541	-0.132	0.019	0.024
6	-0.461	-0.430	-0.376	-0.376	-0.383	0.205	0.066	0.091
7	0.835	0.832	0.796	0.798	0.784	1.035	0.336	0.372
8	0.309	0.191	0.248	0.249	0.260	-0.097	0.235	0.435
9	-0.182	-0.220	-0.183	-0.177	-0.184	0.193	0.210	0.096
10	0.068	0.033	0.055	0.052	0.076	-0.587	-0.061	-0.006
11	0.129	0.028	0.021	0.022	0.014	0.882	0.148	0.135
12	0.157	0.230	0.276	0.284	0.288	-0.464	-0.133	-0.028
13	0.788	0.793	0.832	0.842	0.839	0.848	-0.018	-0.024
14	0.101	0.131	0.146	0.143	0.140	0.195	0.047	0.028
15	0.555	0.483	0.473	0.476	0.466	0.582	0.137	0.214
16	-0.126	-0.123	-0.108	-0.115	-0.102	-0.674	0.077	0.186
17	-0.390	-0.364	-0.389	-0.393	-0.398	0.278	-0.035	-0.013
18	-0.131	-0.166	-0.182	-0.175	-0.182	-0.029	0.233	0.165
19	0.160	0.284	0.288	0.292	0.290	-0.129	0.153	0.133
20	-0.188	-0.066	-0.043	-0.046	-0.033	-0.480	-0.004	0.011
21	-0.135	-0.257	-0.205	-0.198	-0.190	0.027	0.062	0.031
22	-0.140	-0.127	-0.149	-0.155	-0.150	-0.131	0.165	0.135
23	0.110	0.198	0.217	0.216	0.230	0.006	0.132	0.168
24	-0.155	-0.153	-0.141	-0.135	-0.141	-0.145	0.095	0.082
25	0.353	0.301	0.291	0.287	0.298	0.298	0.123	0.145
26	0.367	0.346	0.329	0.329	0.329	-0.067	0.070	0.135
27	-0.302	-0.270	-0.253	-0.244	-0.231	-0.515	-0.059	0.000
28	0.195	0.138	0.129	0.133	0.134	0.065	-0.081	-0.041
29	-0.122	-0.238	-0.211	-0.204	-0.191	0.093	-0.001	-0.011
30	-0.495	-0.534	-0.560	-0.561	-0.562	-0.323	-0.069	-0.091

Table 3. Statistical Values of $N_{GNSS/Lev} - N_{GGM}$ (m)

Compared Models	Min.	Max.	Mean	Std. Dev.	± RMS
GNSS/Levelling-EIGEN-GRGS.RL04	0.495	0.835	0.043	0.348	0.345
GNSS/ Levelling-GO_CONS_GCF_2_DIR_R6	0.534	0.832	0.034	0.346	0.342
GNSS/ Levelling-GO_CONS_GCF_2_TIM_R6	0.560	0.832	0.045	0.348	0.345
GNSS/ Levelling-GO_CONS_GCF_2_TIM_R6e	0.561	0.842	0.046	0.349	0.346
GNSS/ Levelling -GOCO06s	0.562	0.839	0.049	0.348	0.346
GNSS/ Levelling -ITSG-Grace2018s	0.674	1.035	0.054	0.429	**0.425**
GNSS/ Levelling -SSG-UGM-2	0.133	0.648	0.087	0.151	**0.172**
GNSS/ Levelling -XGM2019e_2159	0.091	0.562	0.102	0.145	0.175

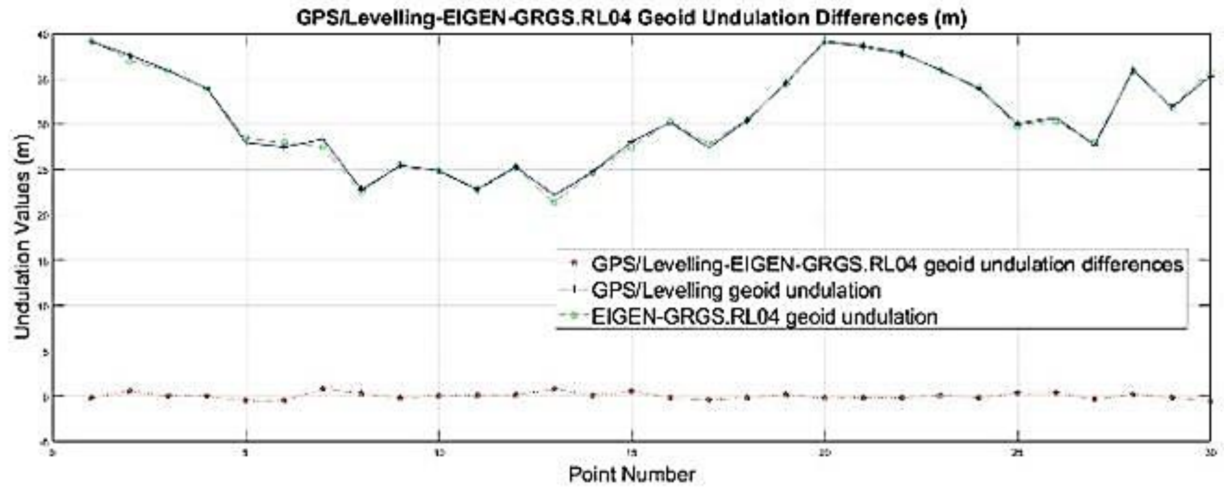

Figure 2. GNSS/Levelling-EIGEN-GRGS.RL04

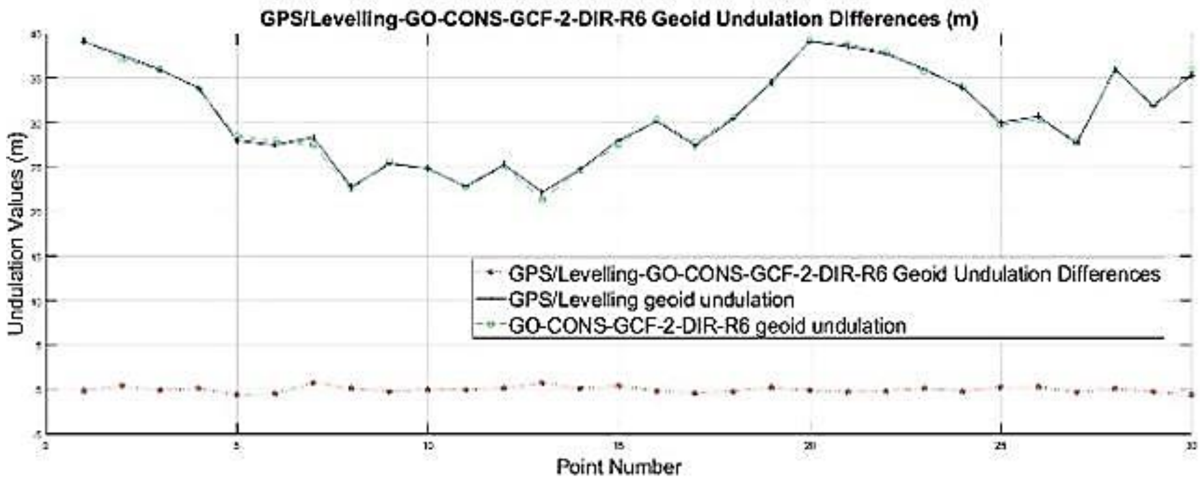

Figure 3. GNSS/ Levelling-GO_CONS_GCF_2_DIR_R6

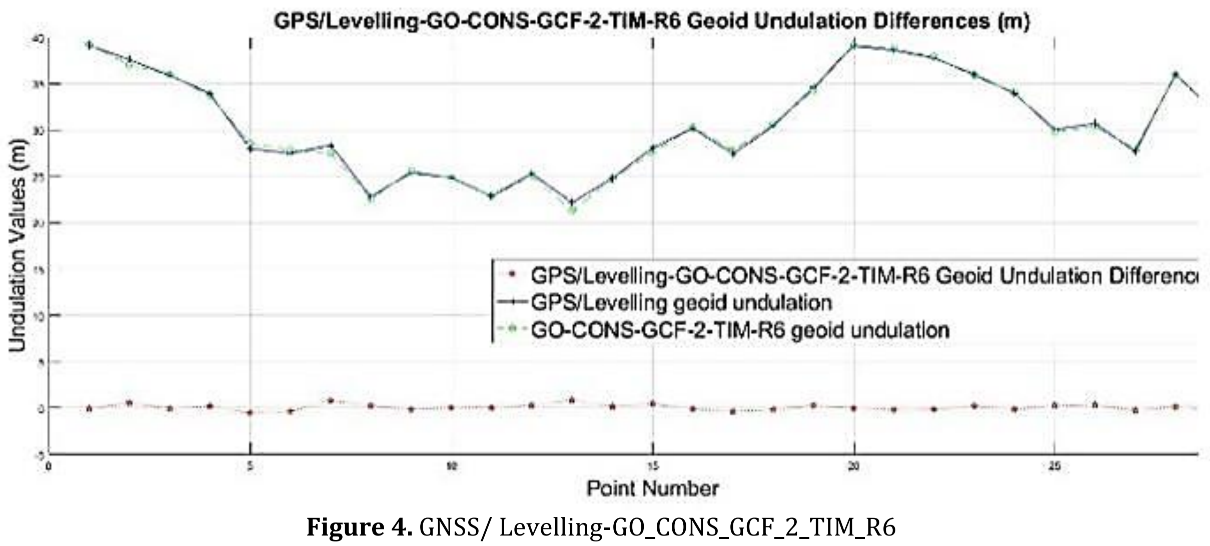

Figure 4. GNSS/ Levelling-GO_CONS_GCF_2_TIM_R6

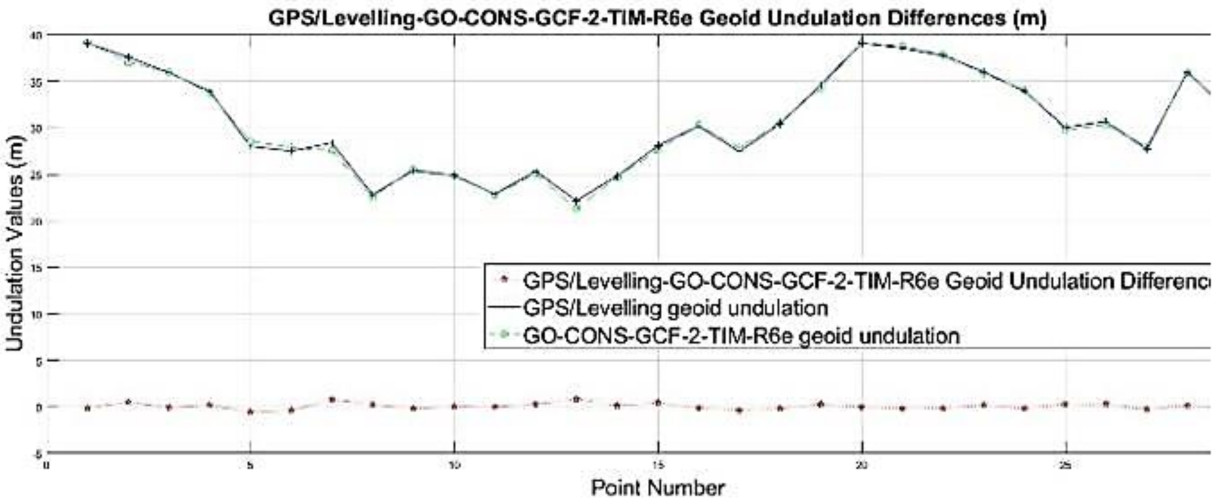

Figure 5. GNSS/ Levelling-GO_CONS_GCF_2_TIM_R6e

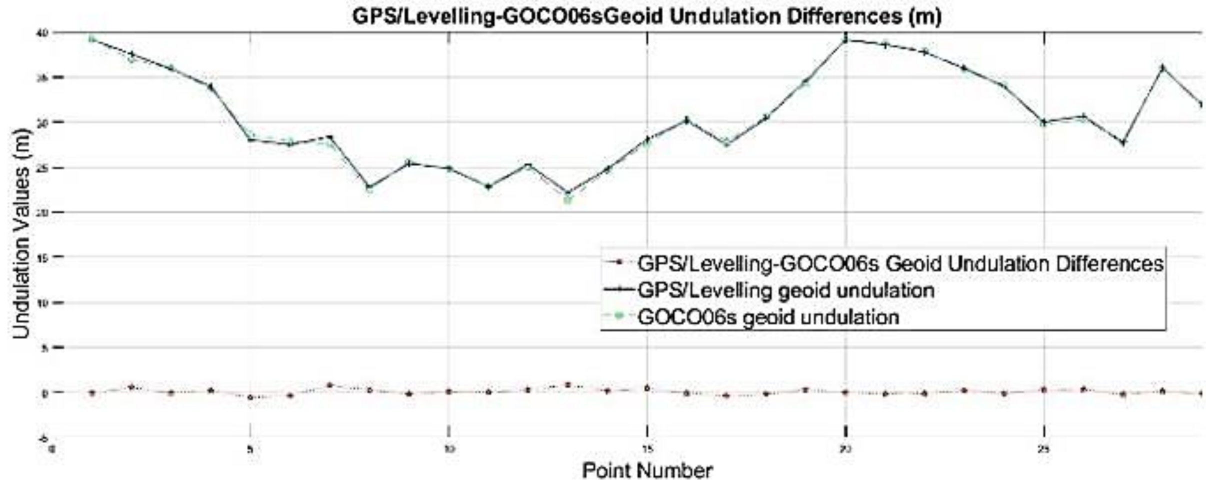

Figure 6. GNSS/ Levelling -GOCO06s

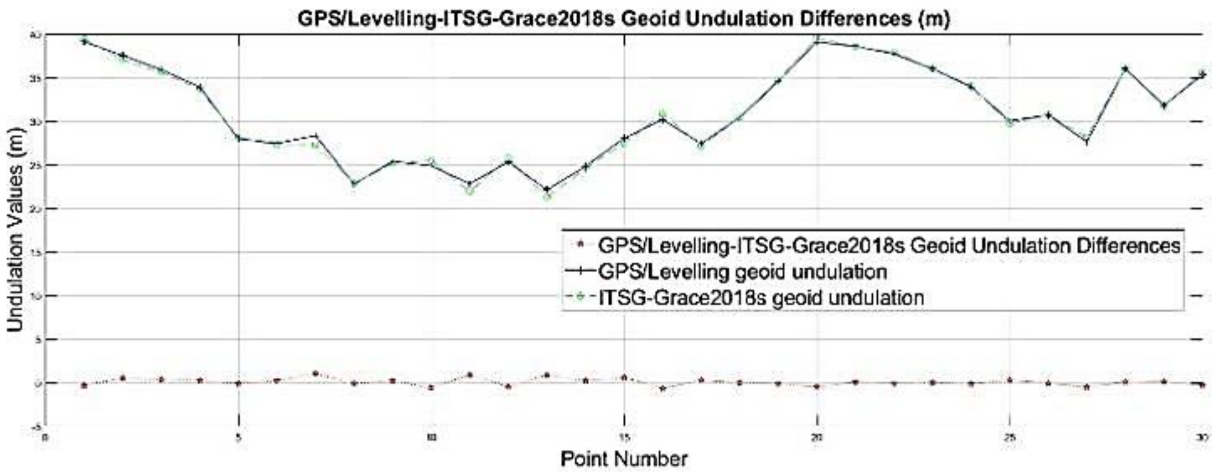

Figure 7. GNSS/ Levelling -ITSG-Grace2018s

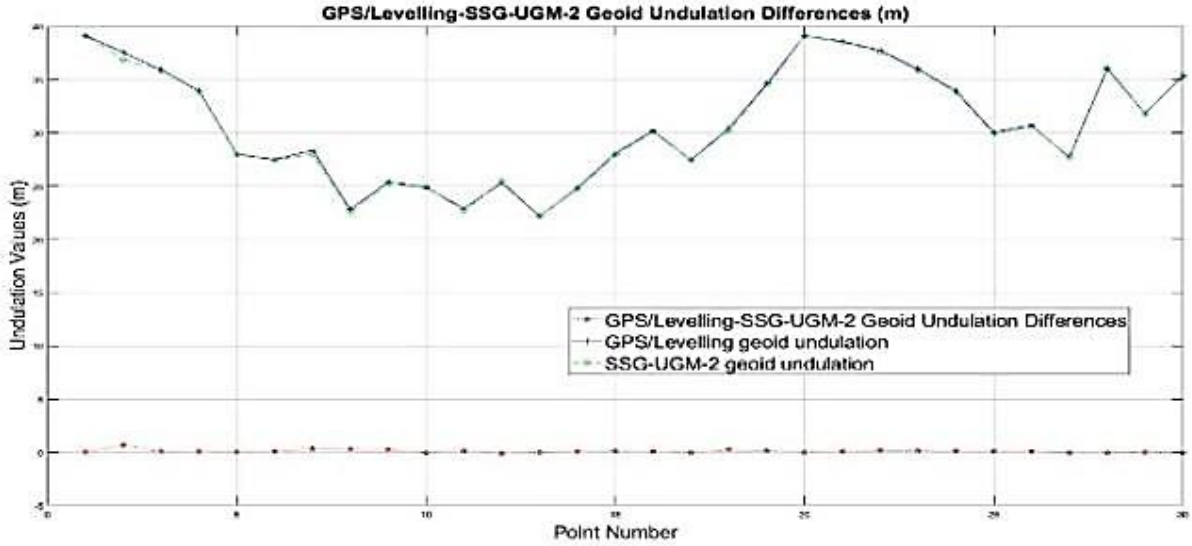

Figure 8. GNSS/ Levelling -SSG-UGM-2

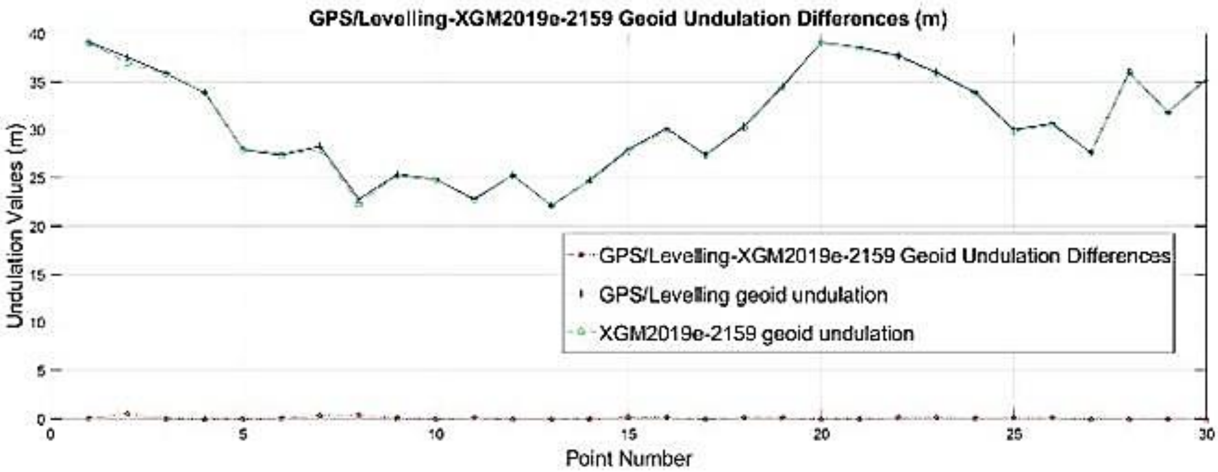

Figure 9. GNSS/ Levelling XGM2019e_2159

4. Conclusion

From the statistical values of the difference of geoid undulations calculated from global geoid models and the geoid undulations calculated from the local GNSS/Levelling geoid (Table 3) at the test points, it was seen that the global geopotential model that deviates the least from the GNSS/Levelling geoid is the SSG-UGM-2 global geoid. The deviation of the local GNSS/Levelling geoid and the SSG-UGM-2 geoid model from each other is approximately 17 cm. The smallest and largest values of the deviation of these two models from each other are approximately 13 cm and 65 cm, respectively. The calculated RMS value for the differences of local GNSS/Levelling geoid undulations and SSG-UGM-2 geoid undulations was found to be the smallest when compared with the calculated RMS values for the differences of other global models from the local GNSS/Levelling geoid. Looking at the criteria based on global geoid models from Table 1, it is seen that the resolutions of these models are different from each other. It is thought that the resolution of the SSG-UGM-2 geoid is much higher than the resolution of other global geoid models, causing this model to better match the local GNSS/Levelling geoid compared to other global geoid models.

From the statistical values of the differences in geoid undulations computed from the global geoid models and the geoid undulations calculated from the local GNSS/Levelling geoid (Table 3) at the test points, ITSG-Grace2018s geoid is the global geopotential that deviates the most from the GNSS/Levelling geoid. The RMS value of the local GNSS/Levelling geoid and ITSG-Grace2018s global geoid comparison is 43 cm. The smallest and largest values of the deviation of these two models from each other are approximately 67 cm and 104 cm, respectively. The calculated RMS value of the differences of local GNSS/Levelling geoid undulations and ITSG-Grace2018s geoid undulations was found to be the largest when checked with the calculated RMS values of the differences of other global models from the local GNSS/Levelling geoid.

It was observed that other global geoid models used in the study could not provide a better fit with Turkey's local GNSS/Levelling geoid than the SSG-UGM-2 global geoid model.

Looking at the compatibility of the GNSS/Levelling geoid and the global geoid models determined in recent years, respectively, are SSG-UGM-2, XGM2019e_2159, GO_CONS_GCF_2_DIR_R6, EIGEN-GRGS.RL04, GO_CONS_GCF_2_TIM_R6, GOCO06s, GO_CONS_GCF_6.

Conflicts of interest

The authors declare no conflicts of interest.

References

1. Apeh, O. I., Moka, E. C., & Uzodinma, V. N. (2018). Evaluation of gravity data derived from global gravity field models using terrestrial gravity data in Enugu State, Nigeria. *Journal of Geodetic Science*, *8*(1), 145-153.
2. Heiskanen, W. A. (1967). Physical geodesy. *Determination of the Geoid from Ground Anomalies*, *8*, 325-330.
3. Yilmaz, M., Turgut, B., Gullu, M., & Yilmaz, I. (2016). Evaluation of recent global geopotential models by GNSS/Levelling data: internal Aegean region. *International Journal of Engineering and Geosciences*, *1*(1), 15-19.
4. El-Ashquer, M., Al-Ajami, H., Zaki, A., & Rabah, M. (2020). Study on the selection of optimal global geopotential models for geoid determination in Kuwait. *Survey review*, *52*(373), 373-382. https://doi.org/10.1080/00396265.2019.1611256.
5. Pavlis, N. K., Holmes, S. A., Kenyon, S. C., & Factor, J. K. (2012). The development and evaluation of the Earth Gravitational Model 2008 (EGM2008). *Journal of geophysical research: solid earth*, *117*(B4). https://doi.org/10.1029/2011jb008916.
6. Liang, W., Li, J., Xu, X., Zhang, S., & Zhao, Y. (2020). A high-resolution Earth's gravity field model SGG-UGM-2 from GOCE, GRACE, satellite altimetry, and EGM2008. *Engineering*, *6*(8), 860-878.
7. Pail, R., Bruinsma, S., Migliaccio, F., Förste, C., Goiginger, H., Schuh, W. D., ... & Tscherning, C. C. (2011). First GOCE gravity field models derived by three different approaches. *Journal of Geodesy*, *85*(11), 819-843. https://doi.org/ 10.1007/s00190-011-0467-x.
8. Save, H., Bettadpur, S., & Tapley, B. D. (2016). High-resolution CSR GRACE RL05 mascons. *Journal of Geophysical Research: Solid Earth*, *121*(10), 7547-7569. https://doi.org/10.1002/2016JB013007.
9. Watkins, M. M., Wiese, D. N., Yuan, D. N., Boening, C., & Landerer, F. W. (2015). Improved methods for observing Earth's time variable mass distribution with GRACE using spherical cap mascons. *Journal of Geophysical Research: Solid Earth*, *120*(4), 2648-2671. https://doi.org/10.1002/2014JB011547.
10. Ince, E. S., Abrykosov, O., Förste, C., & Flechtner, F. (2020). Forward gravity modelling to augment high-resolution combined gravity field models. *Surveys in Geophysics*, *41*(4), 767-804. https://doi.org/10.1007/s10712-020-09590-9.
11. Ogutcu, S. (2020). Performance assessment of IGS combined/JPL individual rapid and ultra-rapid products: Consideration of Precise Point Positioning technique. *International Journal of Engineering and Geosciences*, *5*(1), 1-14.
12. Tusat, E., & Ozyuksel, F. (2018). Comparison of GPS satellite coordinates computed from broadcast and IGS final ephemerides. *International Journal of Engineering and Geosciences*, *3*(1), 12-19.
13. Pırtı, A., Hoşbaş, R. G., Şenel, B., Köroğlu, M., & Bilim, S. (2021). Galileo uydu sistemi ve sinyal yapısı. *Geomatik*, *6*(3), 207-216.
14. Başçiftçi, F. (2021). TUSAGA-AKTİF Noktalarında Gürültü Analizi, Türkiye'nin Güneydoğusu Örneği. *Geomatik*, *6*(2), 135-147.
15. Özdemir, E. G. (2022). Bağıl ve mutlak (PPP) konum çözüm yaklaşımı sunan Web-Tabanlı çevrimiçi veri değerlendirme servislerinin farklı gözlem periyotlarındaki performanslarının araştırılması. *Geomatik*, *7*(1), 41-51.
16. Zingerle, P., Pail, R., Gruber, T., & Oikonomidou, X. (2020). The combined global gravity field model XGM2019e. *Journal of Geodesy*, *94*(7), 1-12. https://doi.org/10.1007/s00190-020-01398-0.
17. Zingerle, P., Brockmann, J. M., Pail, R., Gruber, T., & Willberg, M. (2019). The polar extended gravity field model TIM_R6e. https://doi.org/10.5880/ICGEM.2019.005.
18. Kvas, A., Behzadpour, S., Ellmer, M., Klinger, B., Strasser, S., Zehentner, N., & Mayer-Gürr, T. (2019). ITSG-Grace2018: Overview and evaluation of a new GRACE-only gravity field time series. *Journal of Geophysical Research: Solid Earth*, *124*(8), 9332-9344. https://doi.org/10.1029/2019JB017415.
19. Lemoine, J. M., Bourgogne, S., Biancale, R., Reinquin F., & Bruinsma, S. (2019). EIGEN-GRGS.RL04.MEAN-FIELD – Mean Earth gravity field model with a time-variable part from CNES/GRGS RL04. 25 Years of Progress in Radar Altimetry Symposium, 24-29 September, Portugal.
20. Kvas, A., Brockmann, J. M., Krauss, S., Schubert, T., Gruber, T., Meyer, U., ... & Pail, R. (2021). GOCO06s–a satellite-only global gravity field model. *Earth System Science Data*, *13*(1), 99-118. https://doi.org/10.5194/essd-13-99-2021.
21. Brockmann, J. M., Schubert, T., & Schuh, W. D. (2021). An improved model of the Earth's static gravity field solely derived from reprocessed GOCE data. *Surveys in Geophysics*, *42*(2), 277-316. https://doi.org/10.1007/s10712-020-09626-0.
22. Alemu, E. (2021). Evaluation of GGMs based on the terrestrial gravity disturbance and Moho depth in Afar, Ethiopia. *Artificial Satellites: Journal of Planetary Geodesy*, *56*. https://doi.org/10.2478/arsa-2021-0007.